Effects of refractive-index mismatch on three-dimensional optical data-storage density in a two-photon bleaching polymer

Daniel Day and Min Gu

Reported is an investigation into the effect of spherical aberration caused by the mismatch of the refractive indices between the recording material and its immersion medium on the three-dimensional optical data-storage density in a two-photon bleaching polymer. It is found both theoretically and experimentally that spherical aberration can be compensated for by a change in the tube length at which a microscope objective is operated in recording and reading processes. After compensation for the spherical aberration it is possible to achieve a three-dimensional recording density of 3.5 Tbits/cm^3 for a commercial objective with a numerical aperture of 1.4.

OCIS codes: 210.4680, 210.4681, 180.2520, 180.6900.

1. Introduction

Recently, three-dimensional (3-D) optical data storage has become an active research area[1–6] because of the 3-D imaging ability of confocal microscopy.[7,8] In this case local chemical and physical reactions are needed to record a data bit at a deep depth of a thick material. To achieve a high recording density, one should adopt a light beam with a short wavelength for recording. However, when a beam of light is focused into a volume medium Rayleigh scattering caused by the medium occurs; the shorter the wavelength, the stronger the scattering process. As a result, the energy carried by the recording beam cannot efficiently be transferred to a position deep in the recording medium. For overcoming this problem a two-photon (2-p) process has been employed[9] in which two incident photons of the recording beam of an infrared wavelength are simultaneously absorbed by the recording medium to produce the local physical and chemical reactions. A number of materials, including photochromic,[1,2] photobleaching,[6] photorefractive,[3–5] and photopolymerizable[5] media, have been employed successfully to achieve 3-D optical data storage.

However, the currently achieveable 3-D recording density is far below the possible limit of terabits per cubic centimeter (assume that the volume of recorded bits is 0.5 μm $\times$ 0.5 μm $\times$ 1.0 μm). One of the main reasons for this low density is the mismatch of the refractive indices between the recording material and its immersion medium, resulting in spherical aberration.[10] It has been demonstrated that this aberration source can dramatically alter the distribution of the light intensity in the focal region of a high-numerical-aperture objective and reduce the intensity at the focus.[10]

Spherical aberration can also be caused if an objective is operated at a nondesign tube length.[11–13] For a commercial microscope objective that satisfies the sine condition a change in tube length results in primary spherical aberration only.[12] If this spherical aberration has a sign opposite to that of the spherical aberration caused by the refractive-index mismatch, the net effect of the two spherical-aberration sources can be minimized. This method has been successfully demonstrated in confocal microscopy.[11,13]

The aim of this paper is to explore the effect of spherical aberration resulting from refractive-index mismatch on the 3-D optical data-storage density in a 2-p bleaching polymer block.[6] Compensation for this aberration that is achieved by means of changing the tube length of an objective used for recording and reading 3-D data is also studied. In Section 2 the diffraction pattern in the focal region of an objective is calculated in the presence of refractive-index mis-

The authors are with the Optoelectronic Imaging Group, School of Communications and Informatics, Victoria University of Technology, P.O. Box 14428 MCMC, Victoria 8001, Australia.

Received 8 December 1997; revised manuscript received 8 June 1998.

0003-6935/98/266299-06$15.00/0

match. The 3-D recording data density is accordingly estimated. The compensation for this aberration is investigated in Section 3. An experimental demonstration of the aberration compensation in 3-D recording and reading is described in Section 4.

2. Aberrated Point-Spread Function Inside a Two-Photon Polymer Matrix

When the refractive index of a recording material does not match that of its immersion material, the diffraction pattern in the focal region of an objective is distorted compared with the diffraction-limited pattern made by an objective used in a uniform medium.[14] The distortion derives from the fact that the refraction of a convergence ray depends on the angle of convergence. As a result, a high-numerical-aperture objective suffers from more distortion than a low-numerical-aperture objective. According to results obtained by Torok *et al.*,[10] a 3-D intensity point-spread function (IPSF) for an objective that satisfies the sine condition can be expressed if an incident plane wave is focused from the first medium of refractive index n_1 into the second medium of refractive index n_2, as

$$I(r, z) = \left| \int_0^{\alpha} (\cos \theta_1)^{1/2} \sin \theta_1 (\tau_s + \tau_p \cos \theta_2) \times J_0(krn_1 \sin \theta_1) \exp(i\Phi + ikzn_2 \cos \theta_2) \mathrm{d}\theta_1 \right|^2, \quad (1)$$

where θ_1 and θ_2 are the angles of a ray of convergence in the first and second media, respectively, J_0 is a Bessel function of the first kind of order zero, k is the wave number in vacuum, and r and z are radial and axial coordinates, respectively, with an origin at the focus that would occur if there were no second medium. The term α is the maximum angle of convergence of the objective that is determined by the numerical aperture of the objective, and τ_s and τ_p are the Fresnel transmission coefficients for the s- and p-polarization states,[14] respectively.

In Eq. (1), Φ is given by

$$\Phi = -kd(n_1 \cos \theta_1 - n_2 \cos \theta_2), \quad (2)$$

where d is the distance from the interface of the two media to the diffraction-limited focus.[10] It is clear that the function Φ acts as a spherical-aberration source because of its dependence on the angle θ_1, which leads to distortion of the diffraction pattern. For a given value of d the larger the difference of the refractive indices between the two media, the stronger the effect of the spherical aberration.

It should be pointed out that the vectorial effect has been ignored in Eq. (1), which is equivalent to neglecting the depolarization effect of the objective. This assumption holds for a maximum convergence angle of less than 45°.[7] Even for an objective with a numerical aperture of 1.4, the vectorial effect does not alter the shape of the 3-D IPSF appreciably.

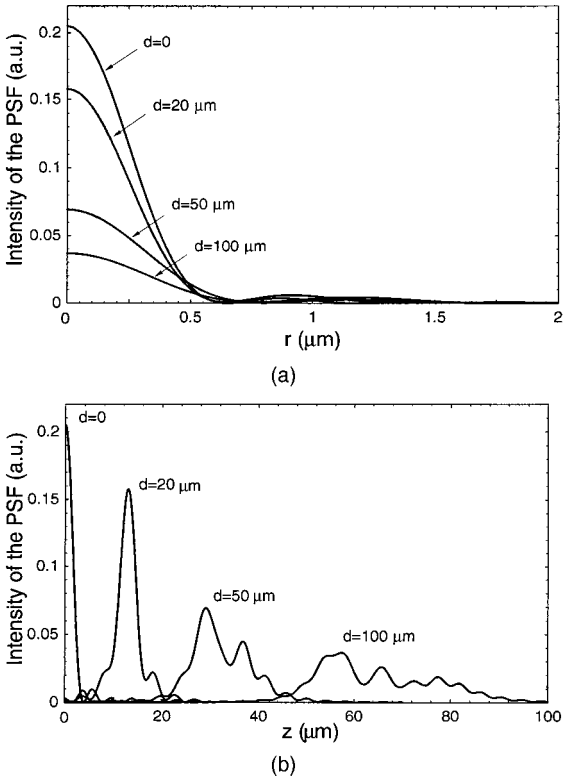

Fig. 1. (a) Transverse and (b) axial cross sections of the 3-D IPSF at different depths in the 2-p bleaching polymer. The objective is assumed to be a dry objective with a numerical aperture of 0.75.

Considering that the working distance of an objective used for recording and reading 3-D data should be long enough to access a deep depth of a volume recording medium, let us take as an example an objective with a numerical aperture of 0.75. The refractive index of the recording material is 1.48 for a wavelength of 798 nm.[6]

For a dry objective, which is more practically relevant to 3-D data storage, the effect of Eq. (2) on the 3-D IPSF within the second medium is shown in Fig. 1. Clearly, the 3-D IPSF at a certain depth of the material is strongly distorted if compared with that at the surface where the effect of Eq. (2) disappears. The solid curves in Fig. 2 show the FWHM's in the transverse and axial directions of the 3-D IPSF as functions of the depth d. It is seen that the FWHM increases appreciably with the depth when d is larger than 40 μm and, in particular, in the axial direction. This phenomenon implies that the 3-D recording density decreases considerably when a laser beam is focused to a position in the polymer deeper than 40 μm. To estimate the recording density, we define the volume of each recorded bit as

$$\Delta V = \frac{4\pi}{3} (\Delta r)^2 \Delta z, \quad (3)$$

where Δr and Δz are the FWHM's of the 3-D IPSF along the radial and axial directions, respectively.

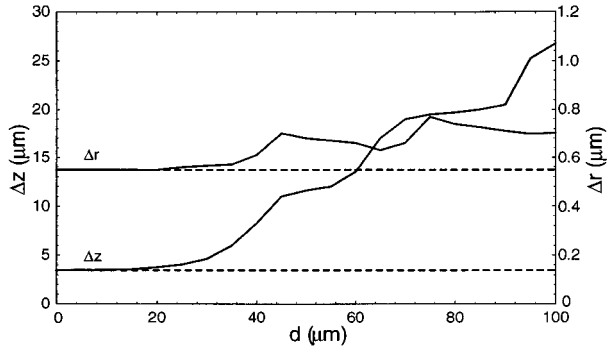

Fig. 2. Transverse and axial FWHM's of the 3-D IPSF's Δr and Δz, respectively, as functions of the depth d of the 2-p bleaching polymer under the unbalanced (solid curves) and balanced (dashed curves) conditions. The objective is assumed to be the same as for Fig. 1.

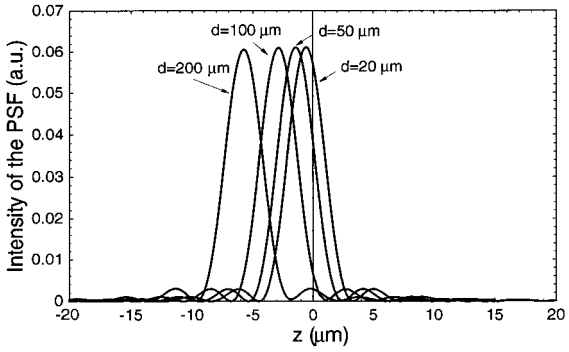

Fig. 4. Axial cross sections of the 3-D IPSF at different depths in the 2-p bleaching polymer. The objective is an oil-immersion objective with a numerical aperture of 0.75.

According to the relation of the FWHM's to the depth d, shown in Fig. 2, the recording density decreases with the depth d. Thus the average 3-D recording density N is given by the integration of $1/(D\Delta V)$ over the depth of a recording material, where D is the thickness of the recording material. For the polymer used, N is approximately 0.05 Tbit/cm^3 for a dry objective with a numerical aperture of 0.75.

The maximum intensity and the focal shift of the 3-D IPSF shown in Fig. 1 are depicted in Fig. 3 as a function of the depth d (see the solid curves). Note that the maximum intensity drops quickly with an increasing depth d. At $d = 40$ μm, it is only 35% of the maximum intensity at $d = 0$. Because the fluorescence intensity under 2-p excitation is proportional to the square of the incident intensity, the 2-p fluorescence intensity at $d = 40$ μm is only approximately 12% of that at $d = 0$. This result means that there is difficulty in recording and reading 3-D data beyond $d = 40$ μm in the polymer if the intensity of the incident laser is kept constant.

The effect of spherical aberration on the 3-D IPSF can be reduced considerably if an oil-immersion objective with a numerical aperture of 0.75 is used, although the use of immersion oil is not practical. In this case the refractive index of the immersion oil is 1.518, and thus the axial FWHM of the 3-D IPSF, shown in Fig. 4, is almost unchanged even at $d = 200$ μm. As a result, the average 3-D recording density can be estimated to be 0.22 Tbit/cm^3, which is 4 times as large as that for a dry objective of the same numerical aperture. Further, the maximum intensity changes by only 0.2% from the surface to a depth of 200 μm.

Although the effect of the refractive-index mismatch can be reduced if an oil-immersion objective is used, the residual mismatch of the refractive indices between the oil and the polymer can still play a significant role if the numerical aperture of the objective becomes large. Figure 5 shows the axial cross section of the 3-D IPSF for an oil-immersion objective with a numerical aperture of 1.4 at different depths of the polymer. It is clear that the axial FWHM of the 3-D IPSF at $d = 100$ μm becomes 3 times as large as that for $d = 0$. A similar effect occurs in the transverse direction. The broadening of the FWHM accordingly results in a reduction of the 3-D recording density. On the other hand, using an oil-immersion objective would not be an applicable method in practical 3-D recording and reading devices because recording materials can be contaminated. Therefore it is necessary to explore an alternative method for reducing the effect of the aberration given in Eq. (2).

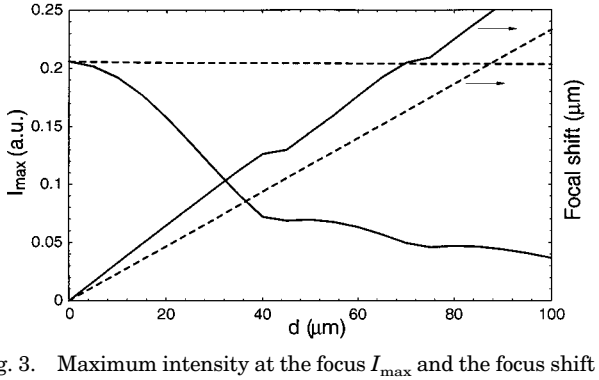

Fig. 3. Maximum intensity at the focus I_{max} and the focus shift z_f as functions of the depth of the 2-p bleaching polymer under unbalanced (solid curve) and balanced (dashed curve) conditions. The objective is assumed to be the same as for Fig. 1.

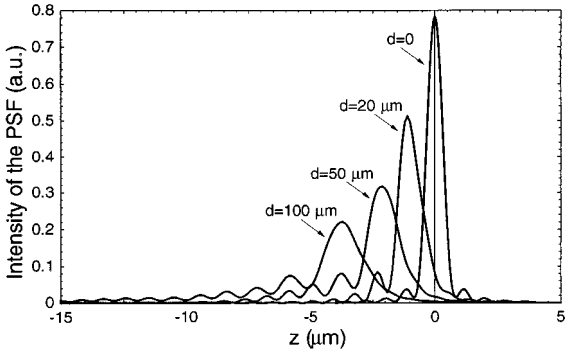

Fig. 5. Axial cross sections of the 3-D IPSF at different depths in the 2-p bleaching polymer. The objective is an oil-immersion objective with a numerical aperture of 1.4.

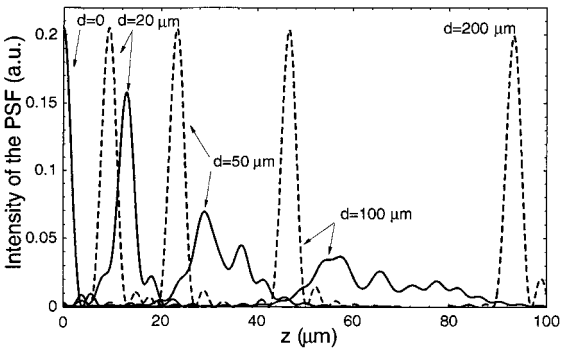

Fig. 6. Axial cross sections of the 3-D IPSF at different depths in the 2-p bleaching polymer under the unbalanced (solid curve) and the balanced (dashed curve) conditions. The objective is assumed to be the same as for Fig. 1.

3. Compensation for Spherical Aberration on the Basis of Variable Tube Length

A commercial objective is designed to operate at a given tube length (the tube length is defined as the distance between an object and its image). For example, in confocal microscopy objectives usually are designed to use a collimated beam, which means that these objectives have an infinitely long tube length,[13] whereas in conventional microscopy objectives usually have a tube length of 160 mm. If the distance between a sample and its image does not satisfy the designed tube length of an objective, spherical aberration can be generated.[11] For a commercial objective that satisfies the sine condition[12,14] the spherical aberration caused by a change in tube length can be described as[12]

$$\Phi_t = B \sin^4(\theta_1/2), \tag{4}$$

which includes only a primary spherical-aberration term. Here B is a parameter related to the wavelength and the magnification of the objective.

By replacing Φ with $\Phi + \Phi_t$ in Eq. (1), we can minimize the effect of the total aberration in Eq. (2) if the sign and the magnitude of B are chosen appropriately to reach a balanced condition between the two aberration sources. Because the 2-p fluorescence intensity is proportional to the square of the incident intensity, the balanced condition of the two aberration sources can be based on the fact that the 3-D IPSF in the polymer reaches the maximum intensity. The 3-D IPSF's for a dry objective with a numerical aperture of 0.75 are shown in Figs. 6, 2, and 3 for the balanced condition given by

$$B = -1.35kd. \tag{5}$$

The negative balanced value of B means that the tube length is increased to compensate for the spherical aberration caused by the air–polymer interface.[12] It can be seen from the dashed curves in Figs. 2 and 3 that both the intensity and the FWHM hardly vary with the depth d under the balanced condition. Therefore the 3-D recording density in this case is approximately 0.22 Tbit/cm^3, as expected. Another important result is that the balanced intensity drops only 0.1% for a depth of as much as 200 μm. These features clearly demonstrate that use of a variable tube length can efficiently reduce the influence of the refractive-index mismatch between the recording material and its immersion medium.

For an oil-immersion objective with a numerical aperture of 1.4 the relation of B to the depth d is slightly nonlinear under the balanced condition. Under the balanced condition the maximum intensity of this objective at $d = 100$ μm is decreased by only approximately 3% compared with that at $d = 0$, and the FWHM almost does not increase. Therefore the average 3-D recording density is approximately 3.5 Tbits/cm^3.

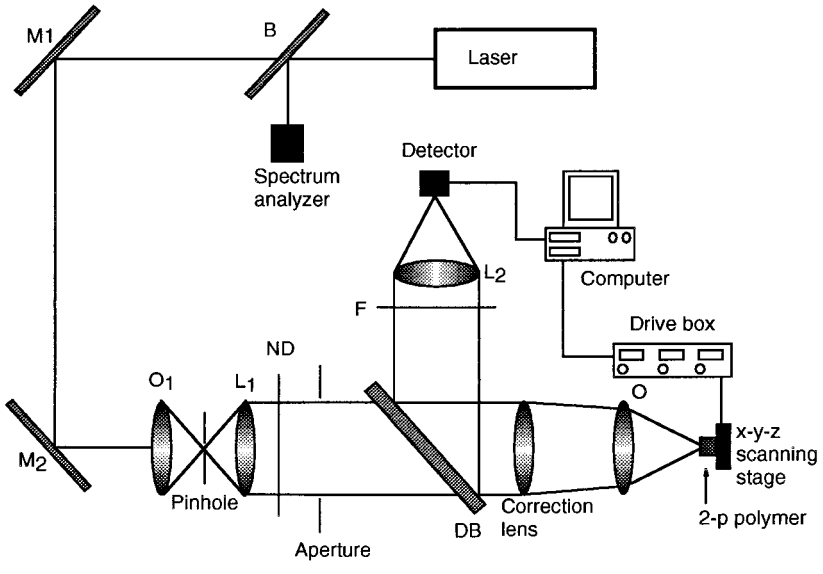

Fig. 7. Experimental setup for recording and reading 3-D optical data in a 2-p bleaching polymer.

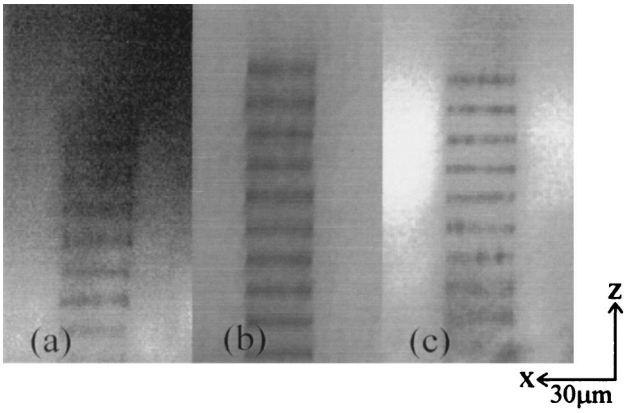

Fig. 8. Recorded 2-p bleached lines with a separation of 10 μm along the axial direction: (a) aberration uncompensated with a dry objective with a numerical aperture of 0.75, (b) aberration uncompensated with an oil-immersion objective with a numerical aperture of 0.75, and (c) aberration compensated with a dry objective with a numerical aperture of 0.75 and a correction lens with a focal length of 300 mm.

4. Three-Dimensional Data Storage in a Two-Photon Polymer Matrix

To demonstrate the effect of the refractive-index mismatch and the mechanism for aberration compensation discussed in Sections 2 and 3, respectively, we performed an experimental study on 3-D recording and reading in a 2-p bleaching-polymer block.[6] Figure 7 is a schematic diagram of an experimental 2-p fluorescence microscope used in recording and reading 3-D data.

The microscope employs a Spectra-Physics Tsunami Model (Ti:sapphire) laser tuned at a wavelength of 798 nm to illuminate a sample. The Tsunami produces 80-fs pulses at a repetition rate of 82 MHz. All mirrors used in the microscope were designed specifically for the ultrashort-pulsed laser. The objective (O_1) (numerical aperture of 0.25) focused the laser beam onto a pinhole to generate a point source, which was then collimated by lens L_1. A neutral-density filter (ND) was used to control the intensity of the incident light during the recording and reading processes. The laser beam was then focused onto a sample by an infinitely corrected objective (O) with a numerical aperture of 0.75 (either an Olympus dry objective or a Zeiss oil-immersion objective). A Melles Griot *x–y–z* translation stage (50-nm resolution) was employed to control the position of the sample. The collected 2-p fluorescence was reflected by a dichroic beam splitter (DB) and focused by lens L_2 onto a photomultiplier tube. A 540-nm short-pass edge filter was inserted in front of the detector to reject the residual signal of the excitation beam. It should be pointed out that the microscope is an object-scanning system that can avoid off-axis aberration. Because of cooperative 2-p excitation, the fluorescence intensity is proportional to the square of the incident intensity. As a result, 3-D imaging is possible without the necessity for a confocal pinhole.[8,9]

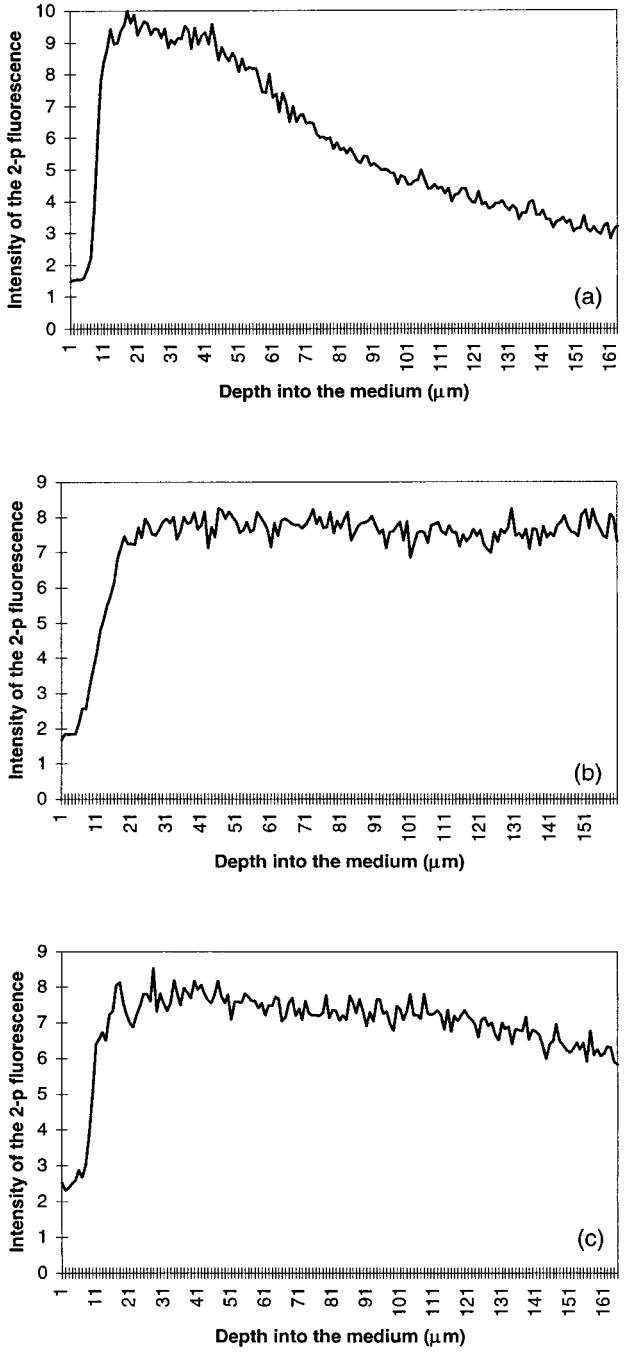

Fig. 9. Axial responses to a thick 2-p bleaching polymer in the reading process: (a) aberration uncompensated with a dry objective with a numerical aperture of 0.75, (b) aberration uncompensated with an oil-immersion objective with a numerical aperture of 0.75, and (c) aberration compensated with a dry objective with a numerical aperture of 0.75 and a correction lens with a focal length of 300 mm.

In the recording process the exposure time for each point of data was approximately 2 s. The average laser power was 7.7 mW and was 0.8 mW for recording and reading, respectively, which gives the same peak intensity in the focus of the objective used in our previous study.[6]

Figure 8 shows a series of bleached lines recorded

in the x–z plane of the polymer with a separation of 10 μm in the z (axial) direction. For the dry objective [Fig. 8(a)] there is no visible bleaching by the seventh line, which corresponds to an axial depth of 70 μm. This result is caused by the dramatic reduction of the intensity in the focus in the presence of the spherical aberration shown in Eq. (1); this result is qualitatively consistent with the theoretical prediction in Fig. 2. If the oil-immersion objective is used [Fig. 8(b)] the bleached lines are clearly visible at a depth of 100 μm compared with the 2-p fluorescence of the background.

According to the balanced condition given in Eq. (5), the spherical aberration caused by the air–polymer interface can be compensated for if the tube length of the objective is increased. To compensate for the effect of the spherical aberration shown in Fig. 8(a), we inserted a positive correction lens with a focal length of 300 mm between the objective (O) and the dichroic beam splitter (DB), so the effective tube length of the objective was increased. Moving the corrective lens to an optimum position at which the 2-p fluorescence is almost constant along the depth of the polymer allows a series of bleached lines to be recorded in the x–z plane of the polymer [Fig. 8(c)]. The line at a depth of 100 μm can now clearly be seen, showing that the spherical aberration caused by the refractive-index mismatch can be considerably reduced by an increase in the tube length of the objective used in recording.

To understand the effect of the spherical aberration on the reading process, we measured the 2-p fluorescence axial responses to the thick polymer block; the results are shown in Fig. 9. For the dry objective [Fig. 9(a)] the fluorescence intensity decreases with the depth d. This behavior is a typical result in the presence of the spherical aberration shown in Eq. (2). At $d = 50$ μm the intensity drops by 50%. This decrease in intensity can be compensated for either by use of an oil-immersion objective [Fig. 9(b)] or by alteration of the tube length of the objective [Fig. 9(c)]. It can be seen that the intensity of the axial response shown in Fig. 9(c) is slightly reduced for a depth of up to 100 μm. This behavior is caused by the fact that the position of the correction lens was fixed at an optimum position. In fact, the correction lens should be moved in step with the objective along the axial direction because the balanced B value is linearly proportional to the probe depth d [see Eq. (5)].

5. Conclusion

It has been shown both theoretically and experimentally that the mismatch of the refractive indices between a volume recording material and its immersion medium can reduce the 3-D data-storage density appreciably along the depth of the material. For a 2-p bleaching polymer,[6] the 3-D storage density can decrease appreciably beyond a depth of approximately 40 μm. The spherical aberration caused by the refractive-index mismatch can be compensated for by an alteration of the tube length of the objective used in recording and reading. This method is also feasible in other applications of 2-p fluorescence microscopy.

The authors acknowledge support from the Australian Research Council and thank S. Schilders for his valuable assistance in operating the ultrashort-pulsed laser (Tsunami). This project also involves a collaboration with P. C. Cheng at the State University of New York at Buffalo, Buffalo, New York.

Address correspondence to M. Gu, Optoelectronic Imaging Group, School of Communications and Informatics, Victoria University of Technology, P.O. Box 14428 MCMC, Victoria 8001, Australia.

References

1. D. A. Parthenopoulos and P. M. Rentzepis, "Three-dimensional optical storage memory," Science **245,** 843–845 (1989).
2. T. Tanaka and S. Kawata, "Randomly accessible, multilayered optical memory with $Bi_{12}SiO_{20}$ crystal," Appl. Opt. **35,** 5308–5311 (1996).
3. Y. Kawata, H. Ueki, Y. Hashimoto, and S. Kawata, "Three-dimensional optical memory with a photorefractive crystal," Appl. Opt. **34,** 4105–4110 (1995).
4. H. Ueki, Y. Kawata, and S. Kawata, "Three-dimensional optical bit-memory recording and reading with photorefractive crystal: analysis and experiment," Appl. Opt. **35,** 2457–2465 (1996).
5. J. H. Strickler and W. W. Webb, "Three-dimensional optical data storage in refractive media by two-photon point excitation," Opt. Lett. **16,** 1780–1782 (1991).
6. P. C. Cheng, J. D. Bhawalkar, S. J. Pan, J. Wiatakiewicz, J. K. Samarabandu, W. S. Liou, G. S. He, G. E. Ruland, N. D. Kumar, and P. N. Prasad, "Two-photon generated three-dimensional photon bleached patterns in polymer matrix," Scanning **18,** 129–131 (1996).
7. T. Wilson and C. R. Sheppard, *Theory and Practice of Optical Scanning Microscopy* (Academic, London, 1984).
8. M. Gu, *Principles of Three-Dimensional Imaging in Confocal Microscopes* (World Scientific, Singapore, 1996).
9. W. Denk, J. H. Stricker, and W. W. Webb, "Two-photon fluorescence scanning microscopy," Science **248,** 73–75 (1990).
10. P. Torok, P. Verga, Z. Laczik, and G. R. Booker, "Electromagnetic diffraction of light focused through a planar interface between materials of mismatched refractive indices: an integration representation," J. Opt. Soc. Am. A **12,** 325–332 (1996).
11. C. J. R. Sheppard and M. Gu, "Aberration compensation in confocal microscopy," Appl. Opt. **30,** 3563–3568 (1991).
12. C. J. R. Sheppard and M. Gu, "Imaging by a high aperture optical system," J. Mod. Opt. **40,** 1631–1651 (1993).
13. C. J. R. Sheppard, M. Gu, K. Brain, and H. Zhou, "Influence of spherical aberration on axial imaging of confocal reflection microscopy," Appl. Opt. **33,** 616–624 (1994).
14. M. Born and E. Wolf, *Principles of Optics* (Pergamon, Oxford, 1980).